SUPPLEMENTARY FIGURES

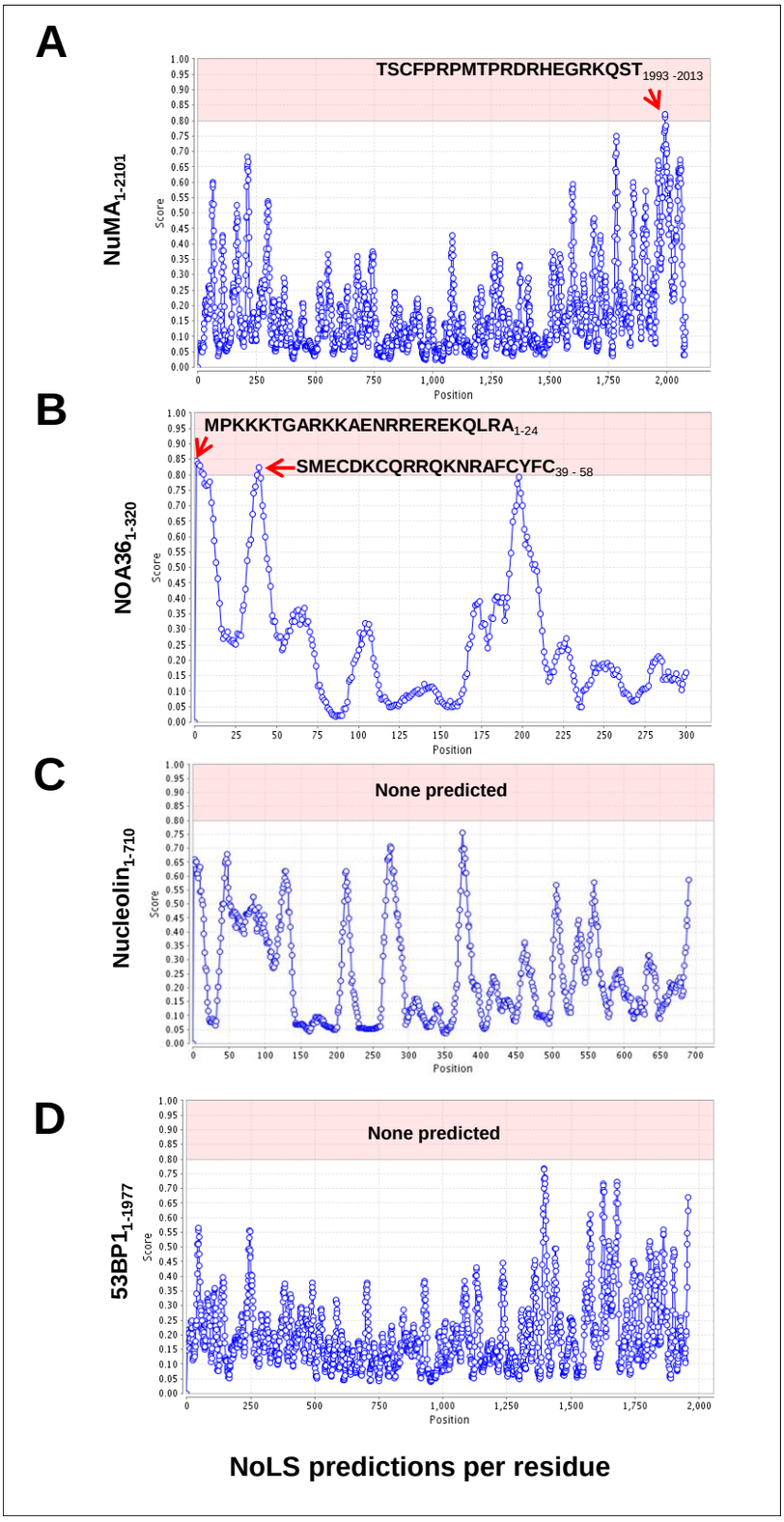

Figure S1. Detection of NoLS regions. The nucleolar localization sequence (NoLS) detector (NoD) web server predicts the presence of NoLS if the average output score of eight consecutive amino acid residues calculated by the artificial neural network (ANN) is at least 0.8. The peaks appearing in the top pink section of the graph as indicated by the red arrows denote potential NoLS residues with the predicted NoLS residues written in black (bold). (**A**) Analysis of the full-length NuMA sequence (residues 1-2101) predicts the presence of a single NoLS in the C-terminus domain between residues 1993-2013. (**B**) Analysis of the full-length nucleolar protein NOA36 (residues 1-320) experimentally shown to contain a highly-conserved NoLS between residues 1-31 [39], predicts the presence of NoLS between residues 1-24 and also between residues 39-58. (**C**) Analysis of the full-length nucleolar marker protein Nucleolin (residues 1-710 with no reported NoLS), and (**D**) analysis of non-nucleolar protein 53BP1 (residues 1–1977; never reported within the nucleolus) do not predict NoLS.

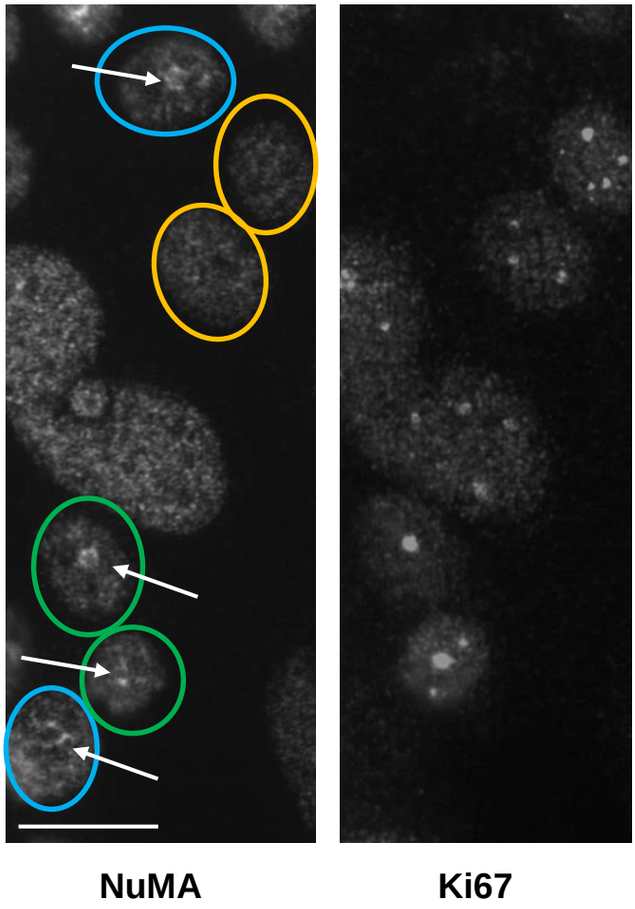

Figure S2. Relationship between the presence of perinucleolar caps for NuMA and cell proliferation. S1 cells were dual-immunostained for NuMA and Ki67 following treatment with 0.08 μg/ml actinomycin D for four hours. Arrows point to nuclei with perinucleolar caps of NuMA. Blue circles denote nuclei with NuMA perinucleolar caps from cells out of the cell cycle (no nucleolar Ki67 staining), green circles denote nuclei with NuMA perinucleolar caps from cells in the cell cycle (nucleolar Ki67 staining), orange circles denote nuclei without NuMA perinucleolar caps from cells in the cell cycle (nucleolar Ki67 staining). Size bar, 10 μm

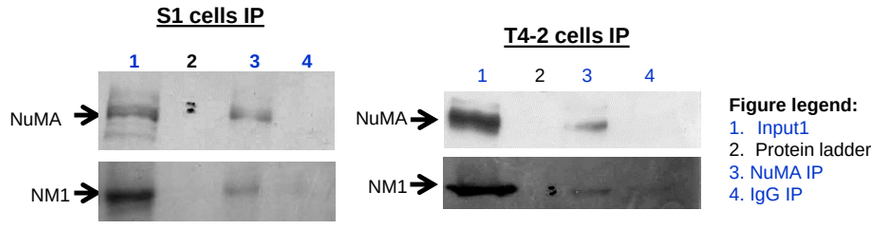

Figure S3A. Uncropped image of Figure 3A, displaying NuMA interaction with B-WICH protein NM1. S1 cells were cultured for eight days with complete medium followed by two days without EGF to induce proliferation arrest. T4-2 cells were cultured for six days. Nuclear extracts were immunoprecipitated with NuMA antibodies (NuMA IP) or nonspecific immunoglobulins (IgG IP), followed by western blot analysis of the input and immunoprecipitated samples for the aforementioned proteins. The membrane was cut into portions with the top and bottom portions probed for NuMA (mouse primary antibody) and NM1 (rabbit primary antibodies), respectively. For the purpose of publication, lanes 1, 3 and 4 (marked in blue) were cropped and presented in Figure 3. Note: we used a precolored ladder that is usually only seen on the transfer membrane.

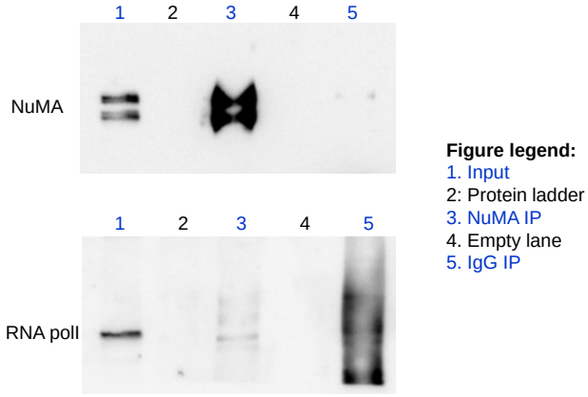

Figure S3B. Uncropped image of Figure 3B displaying NuMA interaction with RNA polymerase I in S1 cells. S1cells were cultured for eight days with complete medium followed by two days without EGF to induce proliferation arrest. Nuclear extracts from S1 cells were immunoprecipitated with NuMA antibodies (NuMA IP) or nonspecific immunoglobulins (IgG IP), followed by western blot analysis of the input and immunoprecipitated samples for the aforementioned proteins. The membrane was cut into two portions, with the top and bottom portions probed for NuMA (mouse primary antibody) and RNA polymerase I (rabbit primary antibody), respectively. Lanes 1, 3 and 5 were cropped and presented in Figure 3. Note: we used a precolored ladder that is usually only seen on the transfer membrane. .

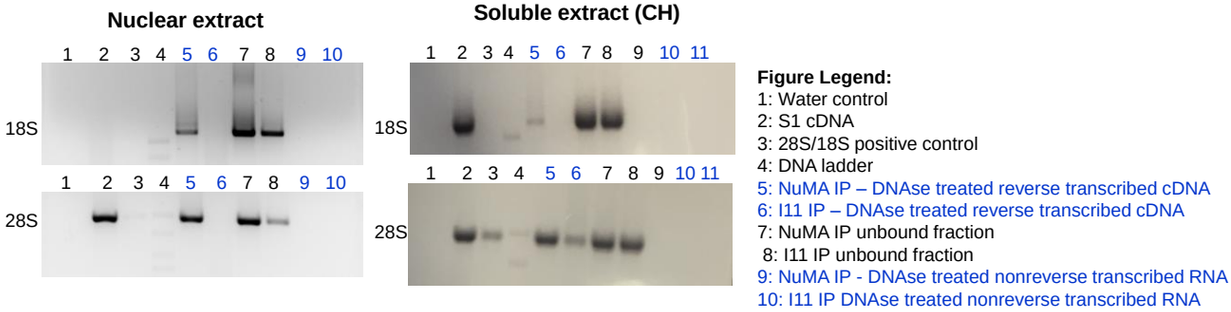

Figure S3C. **Uncropped image of Figure 3D displaying NuMA interaction with 18S and 28s rRNA**. RNA immunoprecipitation from T4-2 cells, with NuMA antibody or with nonspecific IgG (I11), of nuclear extract and 50 mg/ml cycloheximide (CH)-treated soluble extract. The aforementioned samples were loaded on agarose gel and subjected to PCR using primers specific for human 18S and 28S rRNAs. Lanes corresponding to DNAse treated reverse-transcribed cDNA (lanes 5 and 6, shown in blue) and DNAse treated nonreverse transcribed RNA (lanes 10 and 11, shown in blue) obtained from NuMA and IgG IP experiments are presented in Figure 3.

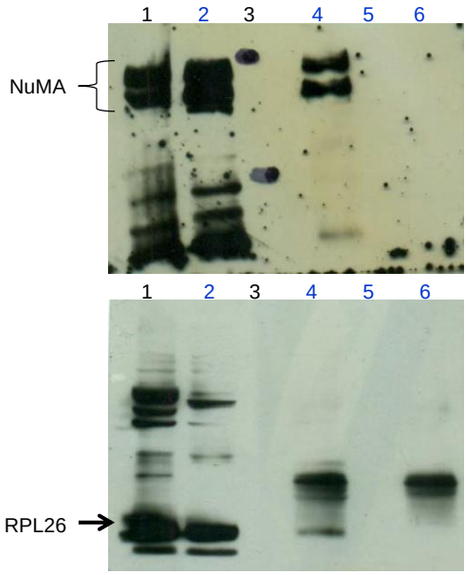

Figure legend:
1. Total protein extract
2. Input
3. Protein ladder
4. NuMA IP
5. Empty lane
6. IgG IP

Figure S3D. Uncropped image of Figure 3E, displaying NuMA interaction with RPL26 in S1 cells. S1 cells were cultured for eight days with complete medium followed by two days without EGF to induce proliferation arrest. Nuclear extracts from S1 cells were immunoprecipitated with NuMA antibodies (NuMA IP) or nonspecific immunoglobulins (IgG IP), followed by western blot analysis of the input and immunoprecipitated samples for the aforementioned proteins. NuMA mouse primary antibody and RPL26 rabbit primary antibody were used on proteins from different gel runs to accommodate for the proteins' molecular weight, and thus gel run conditions, but the immunoprecipitates are the same. Lanes 2, 4, 5 and 6 (marked in blue) were cropped and presented in Figure 3. Heavy (top blue arrow) and light (bottom blue arrow) IgG chains are also seen on the IP lanes.

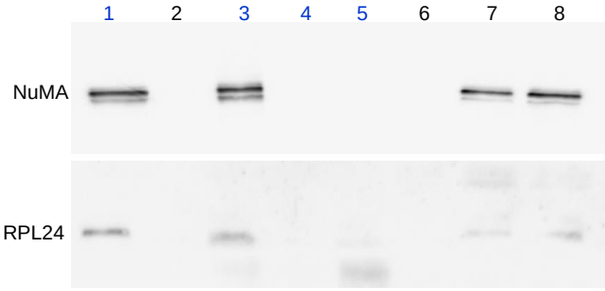

Figure legend:
1. Input
2. Protein ladder
3. NuMA IP
4. Empty lane
5. IgG IP
6. Empty lane
7. NuMA IP unbound fraction
8. IgG IP unbound fraction

Figure S3E. Uncropped image of Figure 3F, displaying NuMA interaction with RPL24 in S1 cells. S1 cells were cultured for eight days with complete medium followed by two days without EGF to induce proliferation arrest. Nuclear extracts from S1 cells were Immunoprecipitated with NuMA antibodies (NuMA) or nonspecific immunoglobulins (IgG), followed by western blot analysis of the input and immunoprecipitated (IP) samples for NuMA (mouse antibody) and RPL24 (rabbit antibody) from different gel runs to accommodate for the proteins' molecular weight, and thus, different gel run conditions, but the immunoprecipitates are the same. Membranes were cut prior to western blots to run western blots for different proteins. Lanes 1, 3, 4 and 5 (marked in blue) were cropped and presented in Figure 3**.**

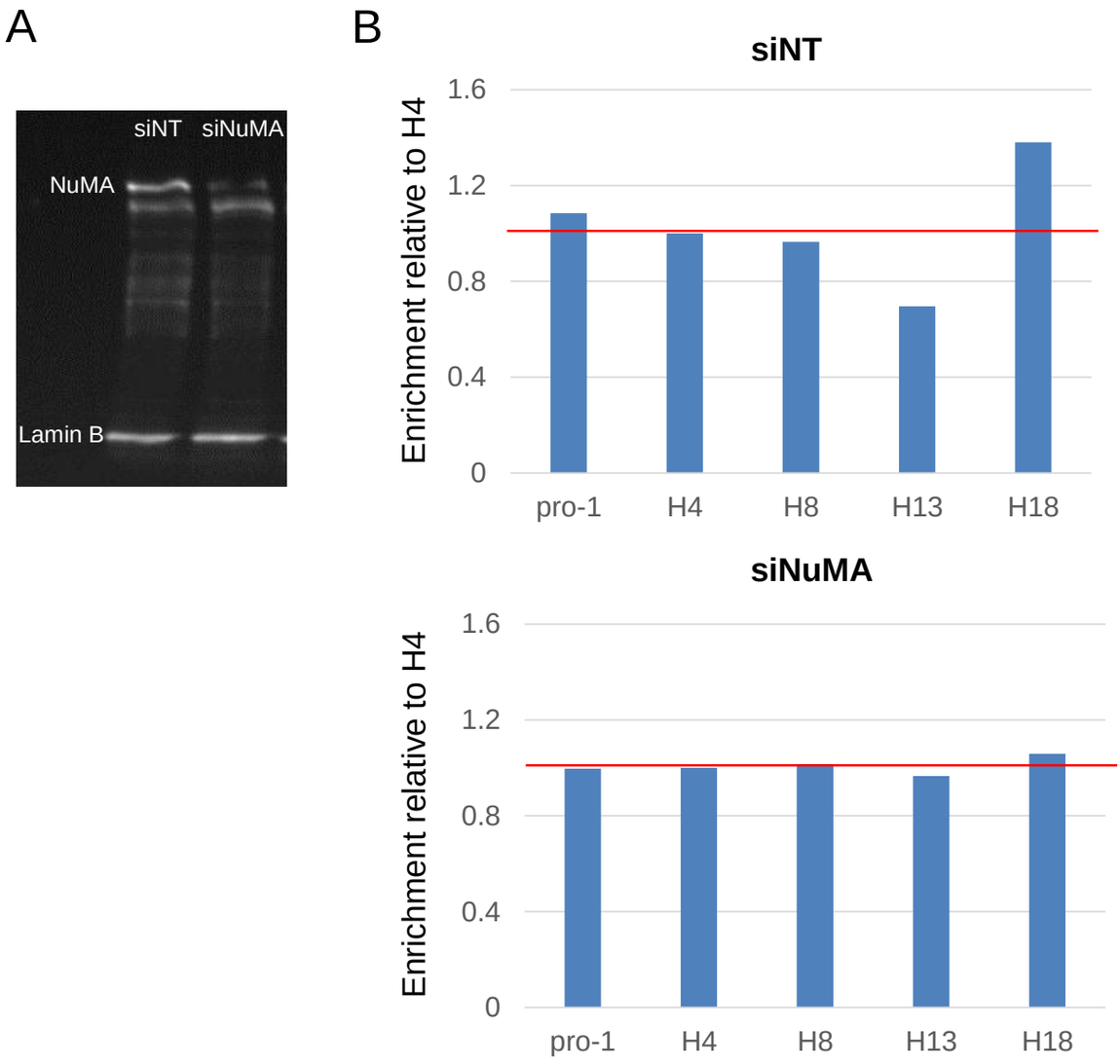

Figure S4. Effect of silencing NuMA on ChIP for rDNA. T4-2 cells were transfected with nontargeting (siNT) or siRNA against NuMA (siNuMA) and prepared for western blot and chromatin immunoprecipitation (ChIP) with NuMA antibody followed by RT-qPCR for coding (pro-1, H4, H8, H13) and noncoding (H18) regions of rDNA. (**A**), western blot for NuMA and loading control lamin B. (**B**) ChIP enrichment data on the graphs are normalized to those obtained with IgG control (see materials and methods) and to H4. The red line corresponds to standardized H4 (=1).

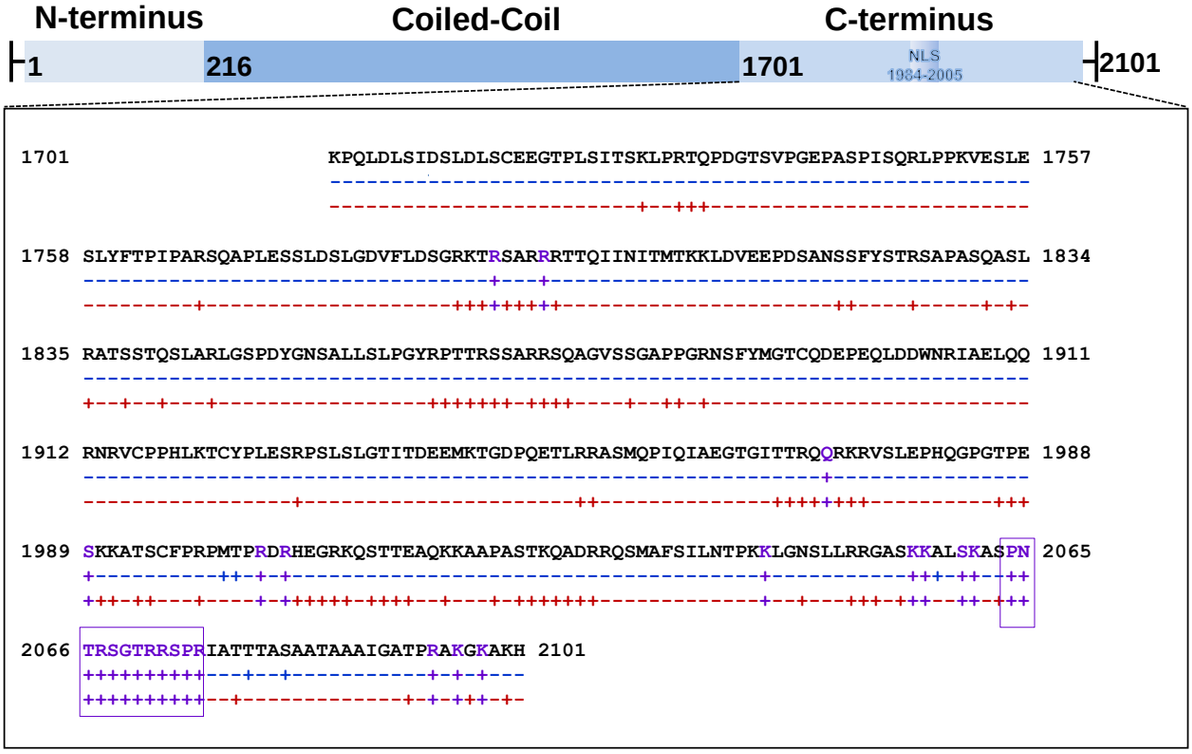

Figure S5. RNABindR and BindN analysis in NuMA. The full length protein sequence of NuMA (residues 1-2101) was analysed using the RNA-based web servers, RNABindR (blue lines) and BindN (maroon lines). Predictions of potential RNA-interacting residues were made using RNABindR and BindN algorithms based on known protein-RNA structures from protein data bank (PDB), with BindN additionally incorporating information obtained from the side chain p(Ka) value, hydrophobicity index and molecular mass of an amino acid. Both servers commonly identified a continuous stretch of 12 amino acid residues (2064-2075) in the CT domain of NuMA (lavender boxes) as potential RNA-interacting residues as indicated by the "+" sign. The "-" sign denotes residues that would not interact with RNA. NLS=nuclear localization signal

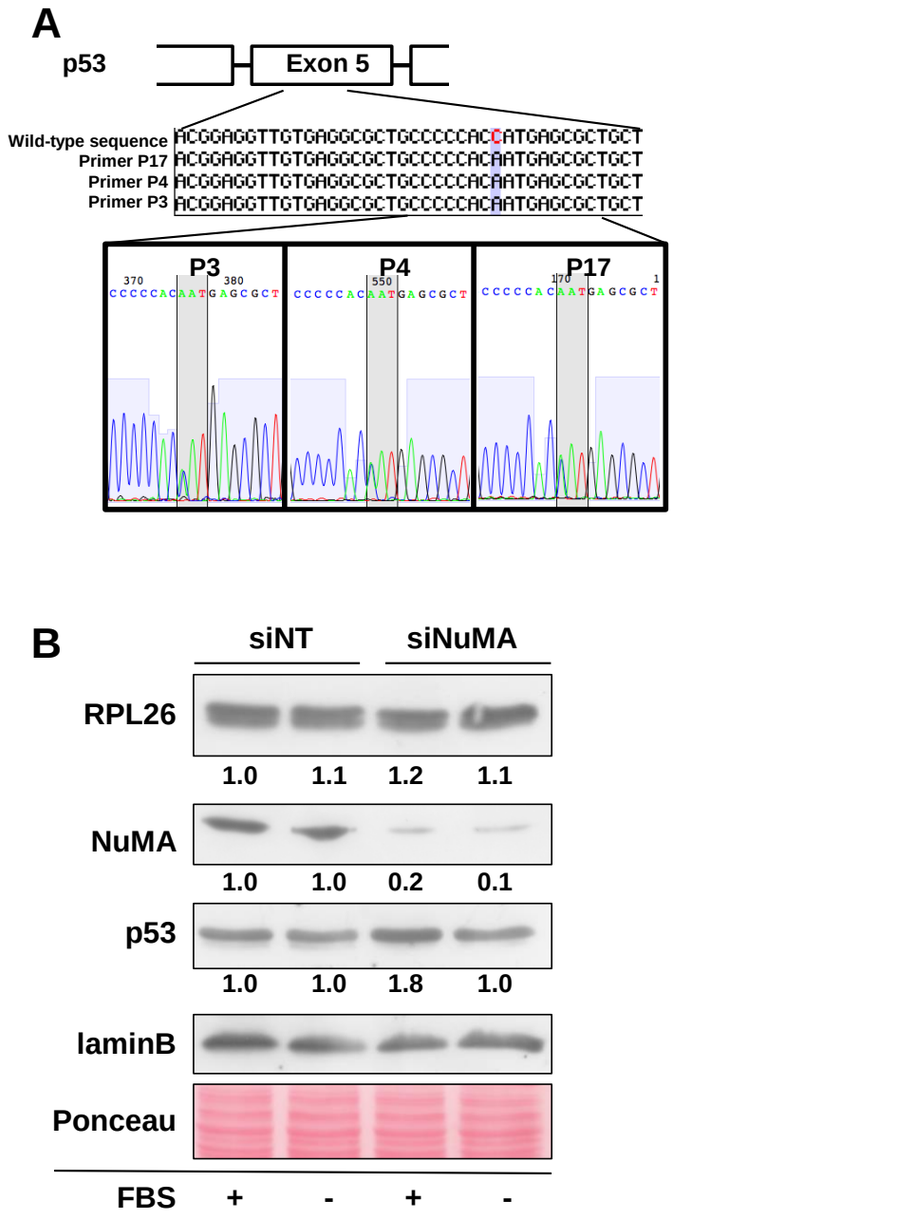

Figure S6. P53 analysis in S1 and MCF7 cells. (**A**) Sequencing of PCR-amplified cDNA for the *TP53* gene in S1 cells (passage 53) with three different sequencing primers P3, P4 and P17. Overlapping cytosine (blue) and adenine (green) traces are consistent with approximately 50% prevalence of the mutation H179N in the cell population. This mutation has been reported to reduce p53 binding to DNA (Ahn et al. (2009). *Cell Cycle*, **10**,1603-1615). (**B**) Western blots and accompanying quantification (compared to the first band of each western blot) for p53, NuMA and RPL26 in MCF7 cells treated with siRNA against NuMA (siNuMA) or with nontargeting siRNA (siNT). Cells were either proliferating (foetal bovine serum [FBS] +) or serum-starved to induce proliferation arrest (FBS -). Ponceau red staining and western blot for lamin B are used as loading controls.

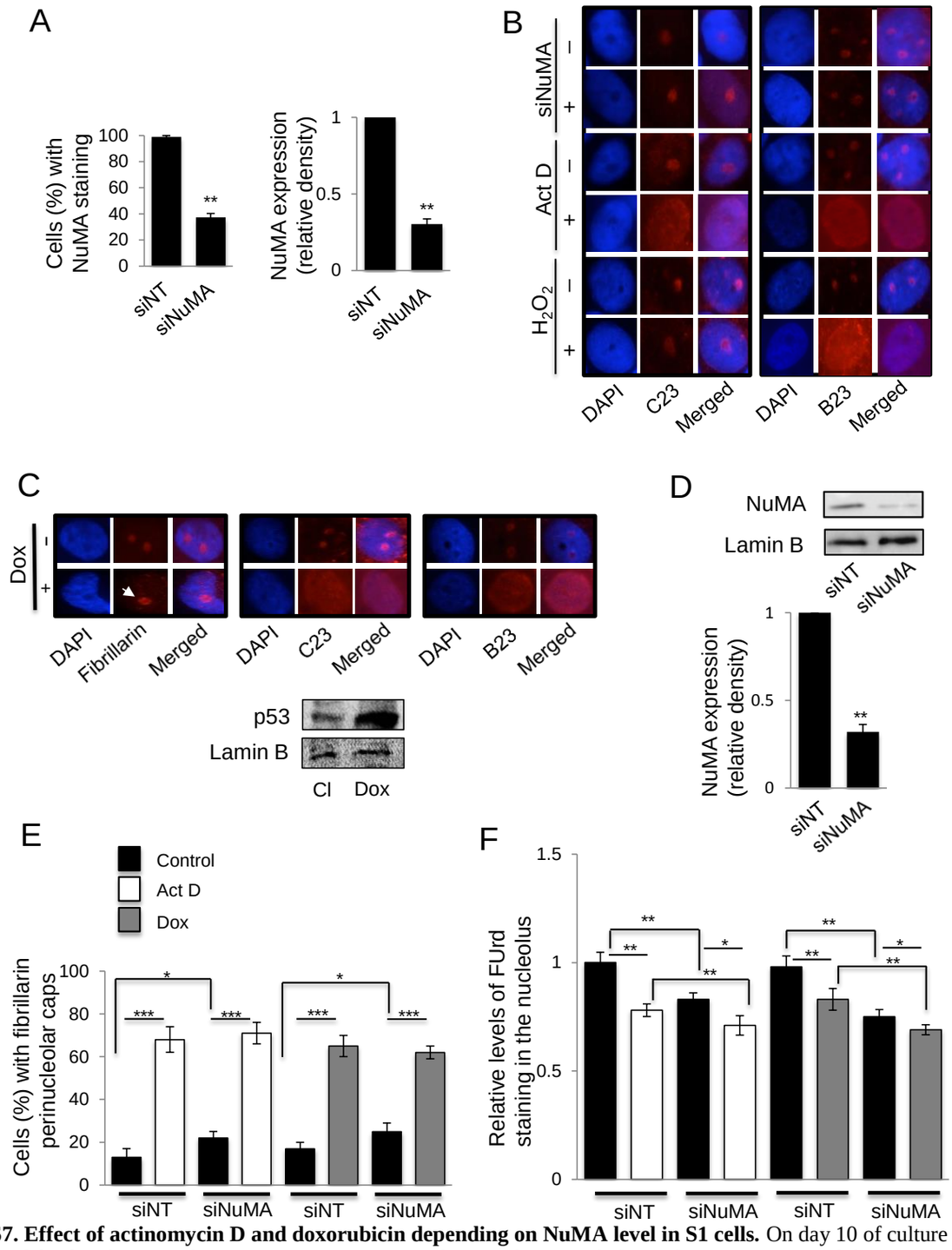

Figure S7. Effect of actinomycin D and doxorubicin depending on NuMA level in S1 cells. On day 10 of culture S1 cells were treated for four hours with actinomycin D (0.08 µg/ml) or six hours with doxorubicin (0.3 µM) and their respective vehicle control (**A**). Quantitative measurement of NuMA levels based on per cell staining (yes or no) and western blot on the cell population for experiments reported on Figure 5; n = 3, >100 nuclei analyzed per replicate. (**B**). Representative immunofluorescence images of nuclei for the distribution of C23 and B23 in S1 cells treated with siRNA nontargeting (siNT), siRNA against NuMA (siNuMA), actinomcycin D (ActD), or H_2O_2 to complement fibrillarin distribution shown on Figure 5B. Nuclei are stained with DAPI (blue). (**C**). Representative immunofluorescence images of nuclei for the distribution of fibrillarin (the arrow shows a perinucleolar ring), C23 and B23, and western blot image of p53 in S1 cells treated with doxorubicin (Dox); Cl = control. Lamin B is used as loading control. (**D**). Representative western blot image of NuMA expression following treatment with siNT and siNuMA for cells used in figures S6 E and F. Graph of quantitative assessment of NuMA protein levels. Lamin B is used as loading control; n = 3. (**E**). Percentage of cells with fibrillarin perinucleolar cap formation under the different treatment conditions (**F**). Levels of FUrd staining for nascent rRNA (nucleolus) following normalization to nucleoplasmic staining intensity (nascent mRNAs) under the different treatment conditions (E&F: n=3; 100 nuclei analyzed per condition; *note*: ActD is a new set of replicates done in parallel with Dox treatment compared to Fig. 5). Statistical analyses were done using one sample t-test for A and D, and multiple-factor ANOVA and Tukey's posthoc test for E and F. **P*<0.05; ***P*<0.01; ****P*<0.001

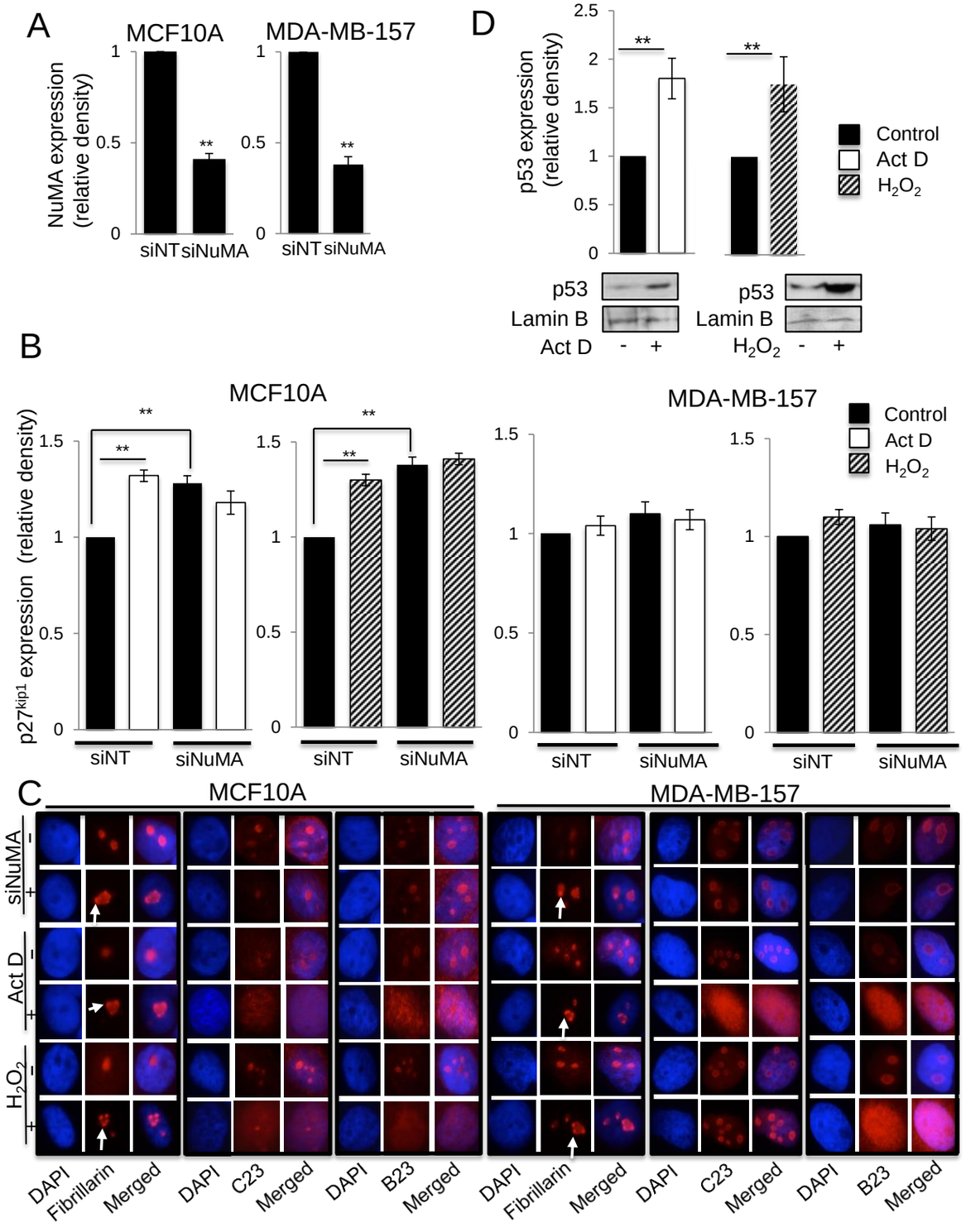

Supplementary Fig S8. Nucleolar stress in WT-p53 and p53-null cells. (**A**). graphs of the level of NuMA expression measured by western blot in siNuMA transfected cells compared to siNT transfected cells (after standardization against internal control lamin B (n=3). (**B**). Levels of $p27^{kip1}$ expression in MCF10A (WT-p53) and MDA-MB-157 (p53 null) cells under actinomycin D (0.08 μg/ml) or H_2O_2 (250 μM) treatment for four hours, relative to siNT control after standardization of $p27^{kip1}$ band against that of internal loading control lamin B (n=3). (**C**). Representative images of cell nuclei stained in red for fibrillarin, C23, or B23. Nuclei are stained with DAPI (blue); arrows indicate perinucleolar caps. (**D**). Graphs of p53 levels in MCF10A cells (we used siNT cells from experiments shown in B and C) following ActD or H_2O_2 treatment (n=3). $^{**}P<0.01$